Supporting Information

One-dimensional DABCO hydrogen-bonding chain in a hexagonal channel of magnetic $[Ni(dmit)_2]$

Simin Li,[a] Kiyonori Takahashi,[a,b]* Ichiro Hisaki,[c] Kenta Kokado, [a,b,d] Takayoshi Nakamura[a,b]*

[a] *Graduate School of Environmental Science, Hokkaido University, N10W5, Kita-ku, Sapporo 060-0810, Japan*
[b] *Research Institute for Electronic Science (RIES), Hokkaido University, N20W10, Kita-ku, Sapporo, 001-0020, Japan*
[c] *Graduate School of Engineering Science, Osaka University, 1-3, Machikaneyama, Toyonaka, Osaka, 560-0043, Japan*
[d] *JST-PRESTO, Honcho 4–1-8, Kawaguchi, Saitama 332-0012, Japan.*

E-mail: (KT) ktakahashi@es.hokudai.ac.jp, (TN) tnaka@es.hokudai.ac.jp

Table of Contents

§1. Experiments

Differential Scanning Calorimetry (DSC)

DSC measurement was carried out with a Q2000 differential scanning calorimeter (TA Instruments) in the temperature range 193-413 K at a heating rate of 5 K ・ min^{-1} and a cooling rate of 5 K ・ min^{-1} under a flow of N_2 gas (flow rate 50 mL ・ min^{-1}).

Powder X-ray diffraction (PXRD) analysis

Powder X-ray diffraction (XRD) patterns were measured with a Rigaku RINT2100 in the 2θ region of 5 - 50°. The measurements were performed with Cu Kα radiation (λ = 1.5418 Å) at scanning rate of 1.2°·min^{-1} under an applied electric voltage and current of 40 KV and 40 mA, respectively.

§2. Thermogravimetry-differential thermal analysis for 1

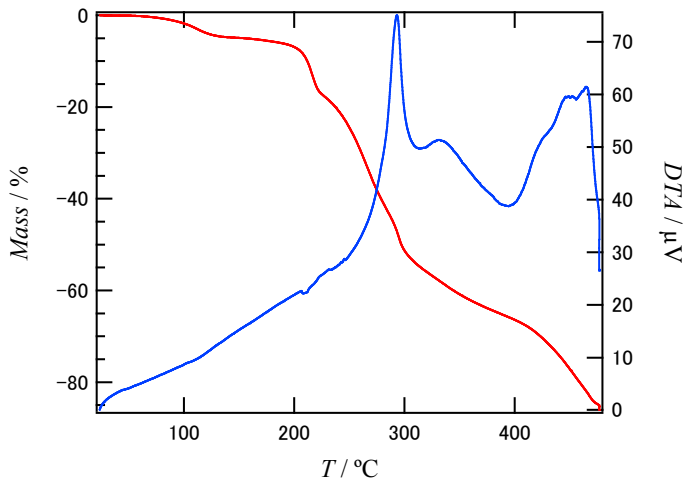

Fig. S1 TG-DTA measurement for crystal **1.** The weight loss at 128 °C was 4.45 % corresponding to 6 molecules of CH_3CN.

§3. Differential scanning calorimetry analysis for 1

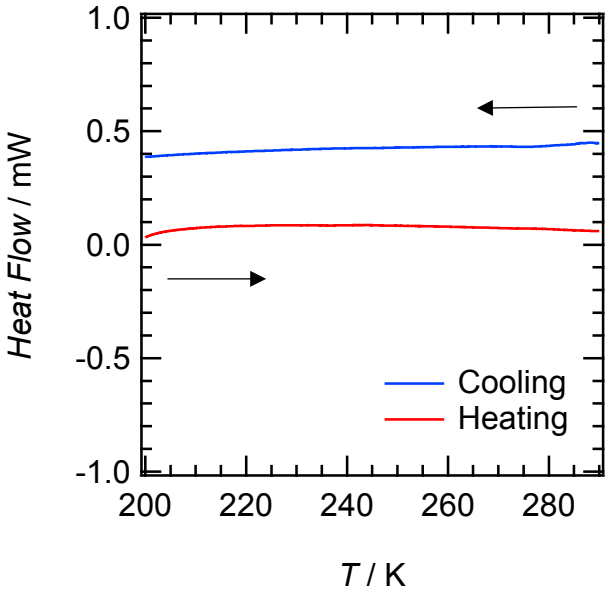

Fig. S2 DSC measurement for crystal **1.** Blue and red lines correspond to cooling and heating cycles, respectively.

§4. Powder x-ray diffraction analysis for 1

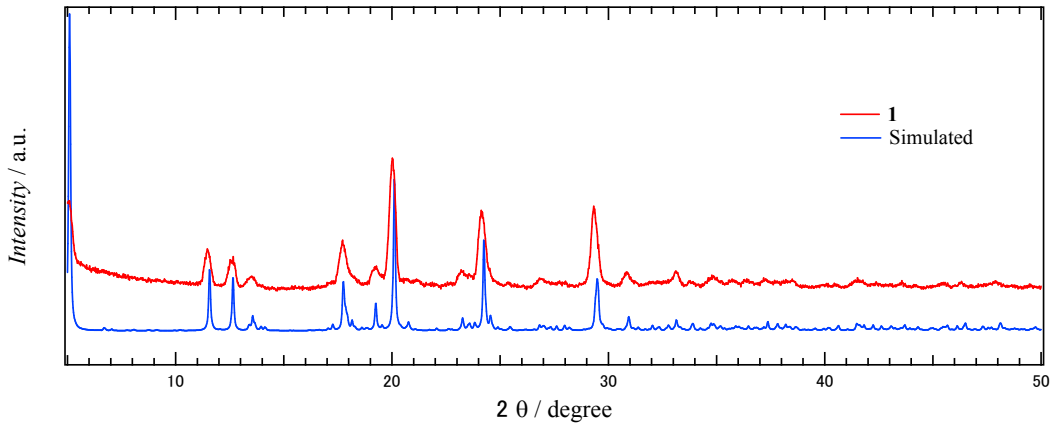

Fig. S3 PXRD measurement for crystal **1.** Simulated pattern was compared to the obtained pattern to confirm the purity of the crystal.

§5. Crystal structure of 1

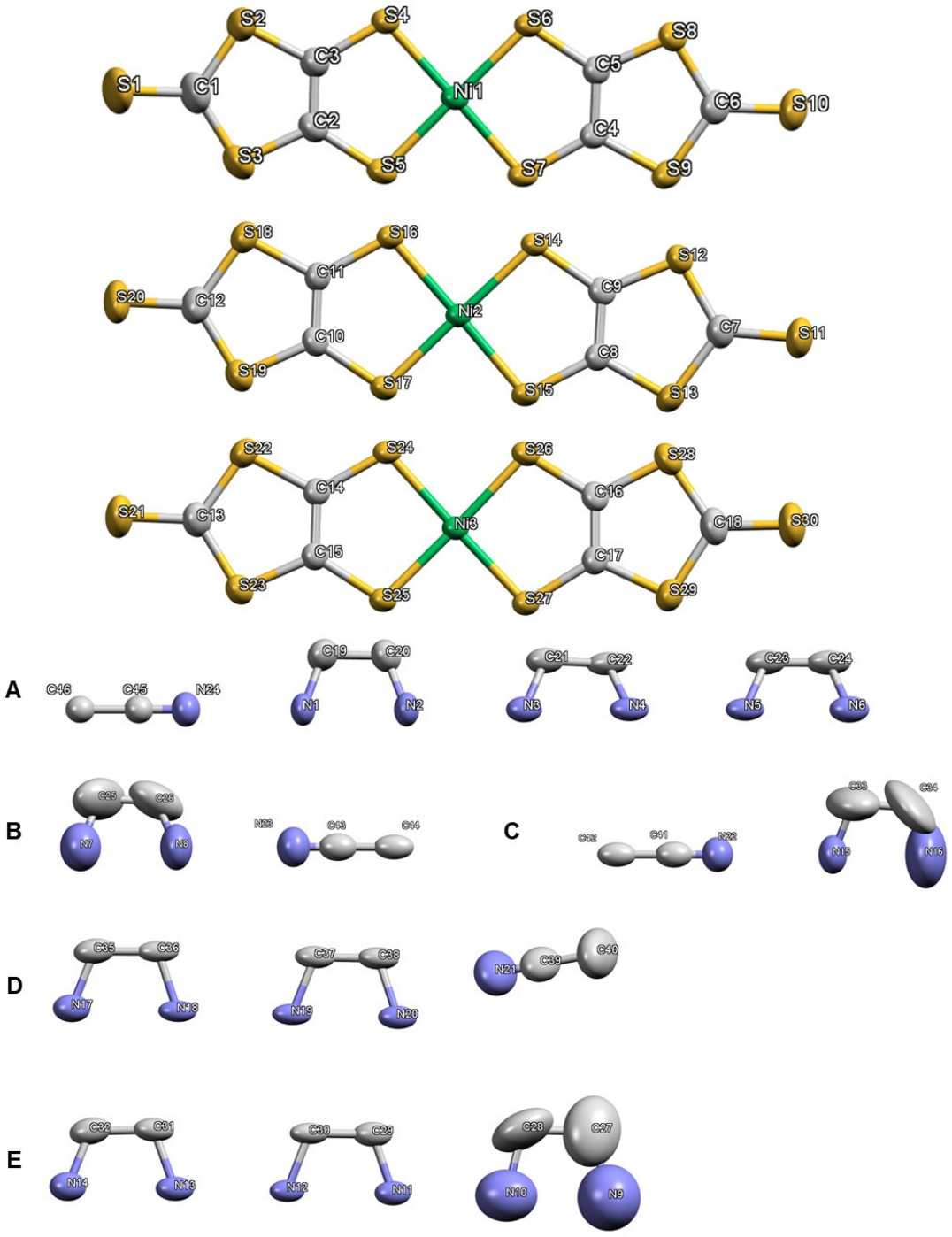

Fig. S4 Crystallographically independent structures of crystal **1** at 173 K. Hydrogen atoms are omitted for clarity. Units **A-E** correspond to hydrogen-bonding units.

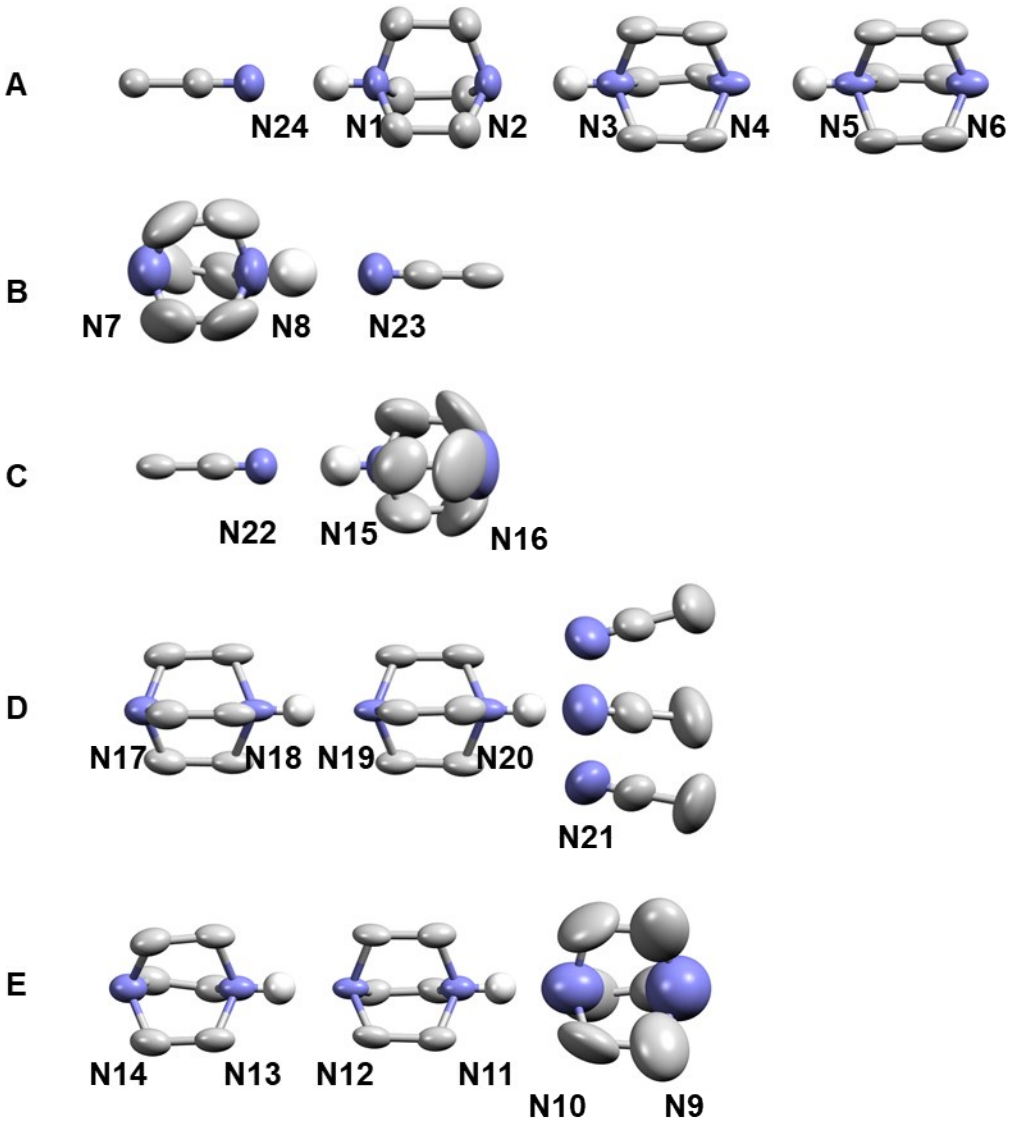

Fig. S5 Hydrogen-bonding units of **A**-**E** at 173 K. The corresponding hydrogen bonding lengths and angles are reported in the Table S1. C, N, and H atoms are depicted in dark-gray, light-blue, and light-gray, respectively.

Table S1. Distances and angles in and between hydrogen bonding units displayed in Fig. S4.

Hydrogen-bonding unit		Distance / Å	Angle / degree
A	N24•••N1	2.856	180
	N2•••N3	2.863	180
	N4•••N5	2.818	180
A•••B	N6•••N7	3.393	---
B	N8•••N23	2.993	180
C	N22•••N15	2.977	180
C•••D	N16•••N17	3.267	---
D	N18•••N19	2.740	180
	N20•••N21	3.000	124.72
E	N13•••N12	2.694	180
	N11•••N10	2.728	180
E•••E	N9•••N9	2.860	---

Hydrogen bond between N20•••N21 consist of one donor and three acceptors. In some cases, this kind of multiple-centered hydrogen bonds has been observed.[S1,S2]

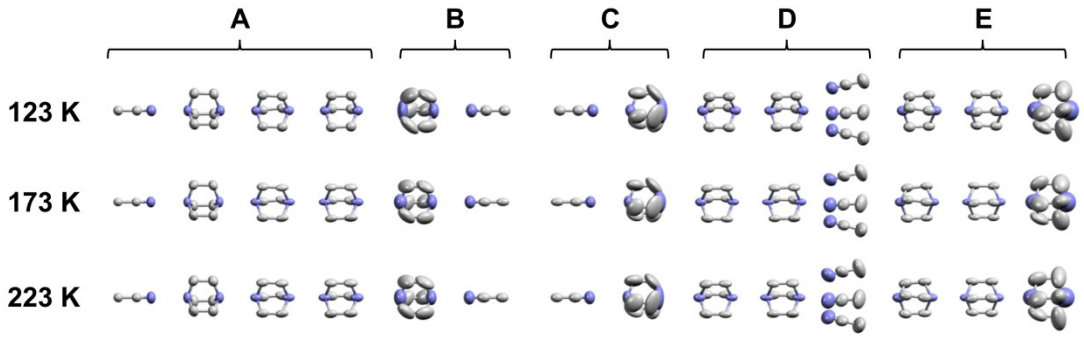

Fig. S6 Temperature-dependence of one-dimensional HDABCO, DABCO, and CH_3CN structures with thermal ellipsoid model with 50% probability.

Table S2. Crystal data, data collection, and reduction parameter for **1** at different temperatures.

Temperature / K	123	173	223
Crystal Dimensions / mm^3		0.196 × 0.144 × 0.065	
Chemical formula		$C_{126}H_{148}N_{26}Ni_9S_{90}$	
Formula weight		5440.49	
Crystal system		*Trigonal*	
Space group		*R*-3	
a, Å	15.1802(2)	15.23710(10)	15.28410(10)
b, Å	15.1802(2)	15.23710(10)	15.28410(10)
c, Å	155.6425(13	155.7837(9)	155.7874(9)
V, $Å^3$	31060.9(9)	31322.5(4)	31516.8(5)
Z		6	
D_{calc}, $g \cdot cm^{-3}$	1.745	1.730	1.720
μ,(Cu K_α) cm^{-1}	9.776	9.694	9.634
$2\theta_{max}$, deg	145.0960	144.6820	144.8880
Reflections measured	68632	32365	74900
Independent reflections	13667	13251	13824
Reflections used	13667	13251	13824
R_1[a]	0.0577	0.0502	0.0420
$R_w(F^2)$[a]	0.1634	0.1401	0.1273
GOF	1.052	1.023	1.031

[a] $R_1 = \Sigma||F_o| - |F_c|| / \Sigma|F_o|$ and $R_w = (\Sigma\omega(|F_o| - |F_c|)^2 / \Sigma\omega F_o^2)^{1/2}$.

§6. Temperature– and frequency–dependent dielectric loss tangent and Arrhenius plot for crystal 1

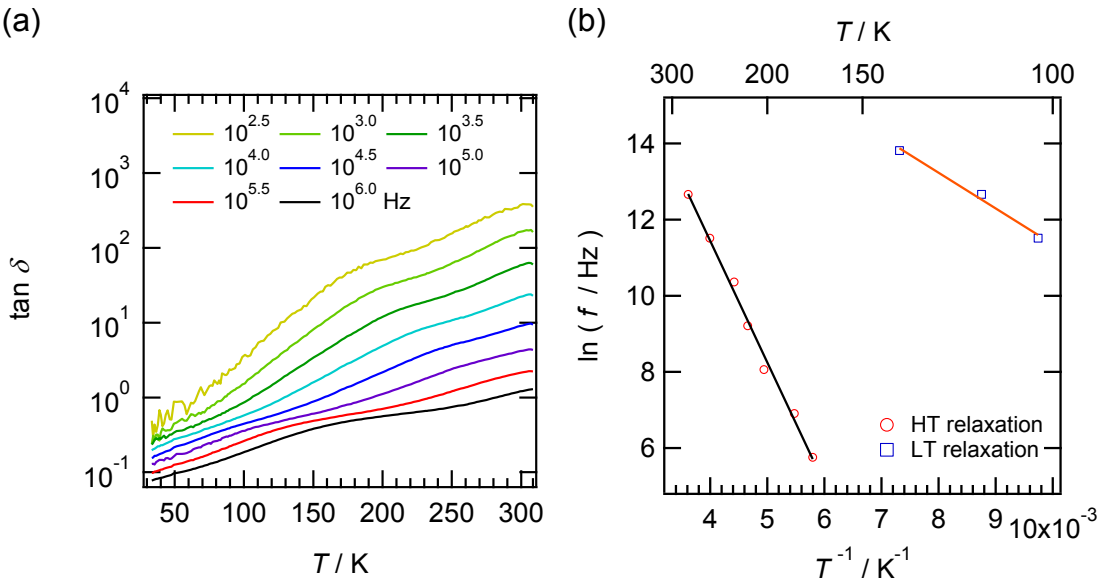

Fig. S7. (a) Temperature and frequency dependent dielectric loss tangent (tan δ), corresponding to ε_1 indicated in Fig. 3(a). (b) Arrhenius plot for the dielectric relaxation frequency (f) of **1** and the respective fits using the Arrhenius law (see text). Red circles and blue squares correspond to relaxation in high temperatures (HT) and low temperatures (LT), respectively.

Arrhenius plot for the dielectric relaxation frequency was given in Fig. S5(b). High temperature (HT) relaxation can be fitted by Arrhenius law with activation energy (E_a) of 26.4 kJ mol^{-1} and pre-exponential factor (f_0) of 2.08×10^{10} Hz, while the best fit for LT relaxation is Arrhenius law with E_a = 7.8 kJ mol^{-1} and $f_0 = 1.01\times10^{9}$ Hz.

§7. References

S1 X. M. Ren, S. Nishihara, T. Akutagawa, S. Noro and T. Nakamura, *Inorg. Chem.*, 2006, **45**, 2229–2234.

S2 G. A. Jeffrey, *An Introduction to Hydrogen Bonding*, Oxford University Press, New York, 1997.